

**Research
Article**

Wake Meandering: A Pragmatic Approach

Gunner C. Larsen*, Helge Aa. Madsen, Kenneth Thomsen and Torben J. Larsen, Wind Energy Department, Risø National Laboratory for Sustainable Energy, Technical University of Denmark, PO Box 49, DK-4000 Roskilde, Denmark

Key words:

wake;
wake meandering;
wake reflection;
wake turbulence;
wind farm;
wind turbine loading;
wind turbine
production

The phenomenon of wake meandering is long known empirically, but has so far not been treated in a satisfactory manner on the wind turbine load modelling side. We present a consistent, physically based theory for wake meandering, which we consider of crucial importance for the overall description of wind turbine loadings in wind farms. In its present version, the model is confined to single wake situations—including a simple heuristic description of wake interaction with a reflecting surface. Contrary to previous attempts to model wind turbine wake loading, the present approach opens for a unifying description in the sense that turbine power and load aspects can be treated simultaneously. This capability is a direct and attractive consequence of the model being based on the underlying physical process, and it potentially opens for optimization of wind farm topology, wind farm operation, as well as control strategies for the individual turbine.

The application of the proposed dynamic wake meandering methodology with existing aeroelastic codes is straightforward and does not involve any code modifications. The strategy is simply to embed the combined effect of atmospheric turbulence, added wake turbulence and the intermittent ‘turbulence contribution’, caused by wake meandering, in files replacing the traditional turbulence file input to aeroelastic computations. Copyright © 2008 John Wiley & Sons, Ltd.

Received 6 July 2006; Revised 25 October 2007; Accepted 22 November 2007

Introduction

Almost from the beginning of the modern wind turbine science development in the late 1970s, there has been a considerable amount of research on wind turbine wakes. For example, several papers on modelling and measuring wake characteristics were presented already in 1980 at the Third International Symposium on Wind Energy Systems, where e.g. the paper of Vermeulen² gives a good overview of the available wake measurements at that time and also presents a description of the main flow mechanisms in the different parts of the wake. A distinct division of the wake into a *near-wake region* (or initial wake region) and a *far-wake region* (or fully developed region) has been used from the beginning of research on wakes and, e.g. introduced by Lissaman.³ In the near-wake region, the flow is complex with the presence of the pressure field from the rotor and distinct vortices from the tip and root of the blades, respectively. Ainslie⁴ gives a detailed description of the near wake and writes that the tip vortices typically have broken down after four diameters, and that the minimum centreline velocity reaches its minimum after one to two rotor diameters. In the far-wake region, the

* Correspondence to: G. C. Larsen, Wind Energy Department, Risø National Laboratory for Sustainable Energy, Technical University of Denmark, PO Box 49, DK-4000 Roskilde, Denmark

E-mail: gunner.larsen@risoe.dk

Contract/grant sponsor: Danish Energy Agency; contract/grant number: ENS 1364/04-0013.

wake profile is typically assumed Gaussian,⁴ and the centreline deficit decays monotonically with a rate strongly dependent on the ambient turbulence, but also on the turbulence generated by the velocity deficit profile itself and the turbulence generated by the mechanical mixing process in the rotor plane. The development of the far wake was modelled with an eddy viscosity model by Ainslie⁴ taking into account the ambient turbulence as well as the deficit-shear-generated turbulence.

The problems and uncertainties, by comparing model results with full-scale measurements, were noticed by Taylor *et al.*,⁵ based on an investigation where model results were compared with wake measurements on the Nibe 630 kW turbines. He describes that the variations in on-site wind direction shift the wake across the downstream rotor disc, and this will increase the average power output from the downstream turbine measured over some time—a mechanism not taken into account in the modelling. Ainslie⁶ discusses the subject in more detail and mentions that wake meandering effects can have considerable influence on *measured* wake deficits, in particular under non-stable atmospheric conditions. It seems that Ainslie⁶ is the first to model the effect from wake meandering on wake deficits by correlating the wake meandering to the variability in the wind direction. In this way, he computes the averaging of wake deficits for two full-scale experiments, and the influence from the meandering is significant in reducing the depth of the deficits.⁶ Further comparisons of model and experimental results, including the correction for meandering for a number of different full-scale experiments, are presented by Ainslie,⁷ and a good correlation between experimental data and model results is found for the centreline velocity deficit decay as function of downstream distance. However, Höglström *et al.*⁸ argued that the applied approach is incorrect, because the variability in wind direction is caused by eddies of all sizes, including those that are smaller than the wake diameter, which the ‘driving’ variability has to be compensated for.

The wake meandering mechanism and its modelling seem not to have been paid much attention in the wake research since the work of Ainslie, but in the concluding remarks in a recent wake review paper of Vermeer *et al.*⁹ on wind turbine wake aerodynamics, it was mentioned that the meandering effect has not yet been satisfactorily modelled. It seems also that some tendencies, in deviations mentioned for different comparisons of model results and full-scale measurements in this review paper, can be ascribed to the effect of meandering. These tendencies are primary: (i) measured velocity deficits are less than computed and (ii) turbulence intensities are higher than computed.

In the present paper, a *model basis* for simulating the wake meandering process is formulated. Significant elements contributing to a full-scale *verification* of various aspects of this theory can be found in Larsen *et al.* [1]. The motivation for formulating the model is, apart from facilitating a correct description of the average wake deficit (as described earlier), at the same time to enable a correct description of the intermittent *dynamic loading* of downstream turbines caused by a meandering wake deficit (potentially including also the associated non-homogeneous modified wake turbulence field). This wake meandering mechanism will not only increase the (apparent) turbulence *intensity*, but may also significantly change the *structure* of the (apparent) turbulence as seen by downstream turbines, and we consider both the correct turbulence intensity and turbulence structure as crucial for correct load prediction.

The wake meandering model is a crucial part of a newly developed *integrated model complex* for performing aeroelastic simulations of a wind turbine subjected to wake conditions. The integrated model complex was presented first time in 2003 by Thomsen *et al.*¹⁰ and Madsen *et al.*¹¹ and later applied to extreme response computation by Thomsen and Madsen.¹² The main mechanism, in the description of the unsteady wake flow in the integrated wake model for aeroelastic computations, is to superimpose the instantaneous wake deficit from the upstream turbine on the undisturbed atmospheric turbulent flow, used as input for aeroelastic simulation of the downstream turbine considered as stand-alone turbine. In this way, the downstream turbine will see as input the (undisturbed) atmospheric turbulence superimposed a wake deficit,* which, because of the mean-

*Note that this is an approximation, as the wake-turbulence field, described in the moving wake frame of reference, will be inhomogeneous with increased turbulence intensity inside the wake boundary and thus differ from that of the undisturbed ambient turbulence field. The meandering wake mean wind speed deficit contribution to the fixed-point turbulence description is, however, considered to be the effect of primary importance.

dering effect, will sweep around in the incoming flow in a plane perpendicular to the mean wind direction, however, most pronounced in the transversal direction. For example, for a 10-min period, where the average wind direction gives half wake operating conditions for the downstream turbine, there will be time periods where the deficit has moved so much in the transversal direction, that the deficit does not interfere with the downstream turbine, and likewise other periods where the downstream turbine will be in full wake. This mechanism will give a significant ‘apparent’ contribution to the turbulence measured at a fixed position corresponding to the location of the downstream turbine, although its origin is basically not traditional turbulence production.

The developed integrated model complex for aeroelastic simulations in wake conditions is thus fundamentally different from the (traditional) approach, where the increased fatigue loading is computed using an increased, effective turbulence in the aeroelastic simulations as, e.g. described by Frandsen,¹³ and which also forms the basis for the recommended method to take into account of wake operation in the International Electrotechnical Commission standard¹⁴ for wind turbines. It is expected that the present new model philosophy can supplement or replace the traditional method, based on an effective turbulence, in a number of different cases as, e.g. in the computation of extreme response in wake operation¹² or in estimation of yaw loading for (partial) wake operation.¹²

Moreover, as the dynamic wake model constitutes a consistent unifying theory for computation of both *power reduction* and *increased loading*, it has also an obvious potential for application in optimization of wind farm topology and wind farm operation, respectively, as well as in optimization of dedicated wind turbines for wind farm applications. Finally, the new model can also be potentially used for development of advanced control strategies for the individual turbine, in order to reduce the blade and turbine fatigue loading during wake operation.

The paper is organized as follows: first, the basic assumptions on which the model is founded are motivated and described. The basic assumptions are followed by a general description of the wake meandering approach. This description is the core of the paper, and it includes an essential low-pass filtering of the stochastic (turbulent) transportation field as well as a model for surface reflection, in case the resulting random walk meandering movement of the wake deficit results in a ‘collision’ with the ground. To make the wake meandering model operational requires selection of specific models for simulation of the wake deficit and the turbulent transportation field, respectively. The implementation chosen for the present application of the meandering model rounds off the model description. Finally, the implications of the model are discussed and conclusions are drawn.

Basic Assumptions

By definition, the displacement pattern of a passive tracer cannot be distinguished from the flow pattern of the flow field responsible for dispersal of the tracer. However, also, flow structures that cannot be characterized as passive, because they vary in their content of momentum compared to the ambient flow (e.g. jets), are known to be affected by the flow pattern of the ambient flow.¹⁵ Guided by such observations, we will consider wake meandering primary to be the result of *large-scale* air movements, in which the turbulent diffusion is of only secondary importance. The *fundamental conjecture* behind the present meandering model is thus that the (transverse and vertical) transport of a wake deficit in the atmospheric boundary layer, in a first-order approach, can be modelled, as if the wake deficit acts as a *passive tracer* despite its content of momentum.

To motivate this basic conjecture heuristically, we consider an idealized situation with a rotationally *symmetrical* wake embedded in a uniform transversal *in-viscous* flow field. We adopt the general hypothesis of dividing the wake into (infinitesimal) elementary parts by plane sections perpendicular to the longitudinal flow direction. Presuming the flow velocity to be constant within each elementary part, we will apply Reynolds transport theorem for momentum on an arbitrary elementary part of thickness dx as illustrated in Figure 1. As no external forcing is applied, because the wake pressure field is presumed symmetric and because the flow is presumed in-viscous, the momentum balance reads¹⁶

$$-\frac{\partial}{\partial t} \iiint_{C.V.} (\rho \mathbf{U}) dV_C = \iint_{C.S.} \rho \mathbf{U} (\mathbf{U} \cdot \mathbf{n}) dS_C \quad (1)$$

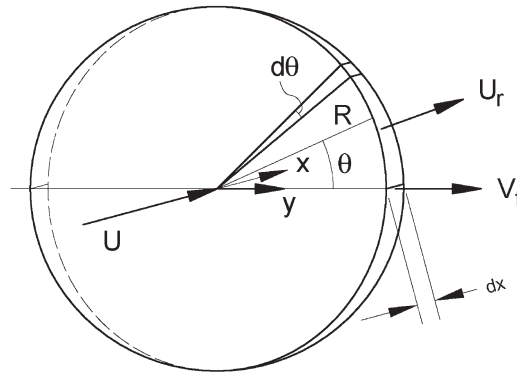


Figure 1. An infinitesimal wake part of thickness dx .

where t is time, $\mathbf{U} = (U, V, W)$ is the fluid velocity relative to an inertial co-ordinate system attached to the control surface (C.S.), ρ is the fluid mass density, \mathbf{n} is the control surface normal, C.V. denotes control volume and dV_C and dS_C are infinitesimal volume and surface elements, respectively.

We define a cylindrical control volume with (arbitrary) radius R and with its axis of symmetry coinciding with the wake symmetry axis. Denoting the rotational symmetric radial velocities induced by the wake by U_r , the uniform transversal flow velocity by V_t and the (constant) velocity of the control volume (i.e. the wake) in the transversal direction by V_w , the momentum balance in the transversal direction is obtained from equation (1) as

$$\begin{aligned} -\frac{\partial}{\partial t} \iiint_{C.V.} (\rho V) dV_C &= \iint_{C.S.} \rho V (\mathbf{U} \cdot \mathbf{n}) dS_C \\ &= dx \rho \int_0^{2\pi} [U_r \cos \theta + V_t - V_w] [U_r + (V_t - V_w) \cos \theta] d\theta \\ &= dx \rho 3\pi U_r (V_t - V_w) \end{aligned} \quad (2)$$

where θ is the angle from horizontal to a point on the control surface, and the homogeneity of the flow density has been utilized.

From equation (2), it is readily seen that *steady conditions* are achieved only when the wake element moves in the transversal direction with a velocity equal to the ambient transversal velocity V_t . Interpreting V_t as resulting from an 'infinite' large turbulent eddy provides the mental link to the adopted fundamental conjecture. It should be noted that for a *viscous* flow, the 'in-balance', caused by a difference between V_t and V_w , will be further strengthened compared to the considered *in-viscous* conditions.

In addition to the basic hypothesis for the transversal and vertical wake deficit displacements, Taylor's hypothesis is adopted for the description of the *downstream advection* of the wake. The downstream advection of the wake deficits is thus presumed to be controlled by the mean wind speed of the ambient wind field. With this formulation, the wake momentum, in the direction of the mean flow, becomes invariant with respect to the prescribed longitudinal wake displacement. This is a considerable simplification allowing for a straightforward *decoupling* of the wake along wind deficit profile (and its expansion) and the wake transportation process.

A precondition for application of Taylor's frozen equilibrium turbulence hypothesis, connecting time and space dimensions, is that the time span considered, T , is *limited* such that variation of the relevant large turbulent eddies, as they move downstream, can be neglected. To justify the adoption of Taylor's hypothesis in the proposed wake meandering theory, we thus implicitly presume the wake deficit dispersions to be associated with time spans complying with such limitations.

This is, however, not a severe restriction, which will be demonstrated in the following. As only large-scale turbulent structures are of importance in a wake meandering context, the relevant turbulent eddies are associated with low wave numbers, k_i , where the subscript ‘ i ’ is referring to Cartesian coordinate axes (along the mean wind direction and in two perpendicular directions). The eddy lifetime, and thus the down wind variation of the turbulent eddies, is considered proportional to $(k_1^2 + k_2^2 + k_3^2)^{-2/6}$,¹⁷ showing that, within the same time span, large eddies are changing considerable less than small eddies. As a consequence, the imposed time span limitation is not considered to result in severe constraints on time spans of practical relevance for the wake meandering process. This is because relevant time spans, by means of Taylor’s hypothesis, is closely related to the down wind spacing of the wind turbines which is in any case limited compared to the spatial scale of the driving turbulent eddies.

However, even with negligible downstream variation of the large-scale eddies, the application of Taylor’s hypothesis is not straightforward. As the atmospheric boundary layer is characterized by a mean *wind shear*, a suitable definition of a characteristic/effective *transport velocity* in the Taylor sense may prove difficult to put forward,^{18,19} since parts of the turbulence structures are likely to move at different velocities as the structure evolves. Hence, only overall convection velocities in a statistical sense may be relevant. In the present context, we, rather arbitrarily, select an average of the ambient mean wind field over the rotor plane as the transport velocity in the Taylor sense. Something similar is suggested in Mann.¹⁷

Meandering Model

Based on the introductory considerations, a pseudo-Lagrangian approach is proposed for the description of the meandering mechanism, in which the stochastic $U + u$ (along wind) component of the spatial velocity field is replaced by a *constant* field mean wind speed U , and where the time evolution of the involved large eddy turbulent structures is neglected. Replacement of $U + u$ with U is a simplification of the problem, and in an average sense it is indeed correct.

In relation to wind turbine loading, the wake deficit movements in the plane perpendicular to the mean wind direction are the ones of primary importance. The size of these transverse movements is *not* affected by neglecting the displacement effect caused by the longitudinal turbulence component, u , but the time scale of the transverse movements are potentially affected. In a loading sense, this is, however, considered a second-order effect, which is further supported by the fact that significant differences between Lagrangian time scales and Eulerian time scales (defined in a frame of reference moving with velocity U) have not been identified from atmospheric measurements.²⁰

When the time evolution of the turbulent structures is neglected, the turbulence is stationary, and as the turbulence is presumed advanced with the (constant) velocity U , Taylor’s hypothesis applies, and the turbulence will automatically be homogeneous in the mean wind direction.²⁰

Pseudo-Lagrangian Approach

When Taylor’s hypothesis applies, a simple transformation between the time dimension and the along-wind spatial dimension exists. As a consequence, a snap shot (associated with a specified time instant t_0) of a spatial turbulence box contains all relevant information of the turbulence in a cross section (perpendicular to the mean wind direction) during a time span $T = L/U$, where L is the along-wind length of the turbulence box, and U is the mean wind speed.

Let us now assume that a wake deficit is ‘released’ from the wake generating rotor at time t_0 , and let t_0 be associated with the turbulence wind field at right bounding *vertical plane* of the turbulence box moving from left to right with velocity U as illustrated in Figure 2.

Let the spatial position of the wake deficit centre be described in an inertial Cartesian coordinate system, fixed to the ground, with the coordinates x^g , y^g and z^g directed in the mean wind direction, the transversal direction and the vertical direction, respectively. For convenience, we define the initial position (at the release time) of the wake deficit centre to $(x^g, y^g, z^g) = (0, 0, 0)$.

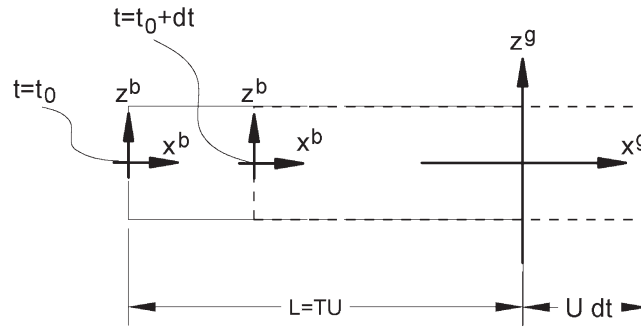


Figure 2. The inertial ground coordinate system (indicated by superscripts 'g') and the (inertial) turbulence box coordinate system (indicated by superscripts 'b')

During an infinitesimal time increment, dt , the turbulence box is advected the distance Udt in the along-wind direction, and the x^g coordinate of the wake centre at time $t_0 + dt$ is thus $x^g = Udt$, where the displacement contribution from the along wind turbulence component are neglected for simplicity* as noted in section *Basic Assumptions*. Let the wake deficit displacement in the vertical (y^g, z^g) plane be described by *characteristic velocities* $v_c(x^b, y^b, z^b)$ and $w_c(x^b, y^b, z^b)$, where the Cartesian (x^b, y^b, z^b) inertial coordinate system is fixed to the turbulence box and related to the (x^g, y^g, z^g) coordinate system at time $t_0 + dt$ as

$$\begin{pmatrix} x^g \\ y^g \\ z^g \end{pmatrix} = \begin{pmatrix} x^b + U[dt - T] \\ y^b \\ z^b \end{pmatrix} \quad (3)$$

For the wake deficit released at time t_0 , the characteristic velocities are given by $v_c(x^b, y^b, z^b) = v_c(UT, y^b, z^b)$ and $w_c(x^b, y^b, z^b) = w_c(UT, y^b, z^b)$. The transversal and vertical positions of the wake deficit centre at time $t_0 + dt$ are thus given by $y^g = v_c(UT, 0, 0)dt$ and $z^g = w_c(UT, 0, 0)dt$, respectively.

More generally, the accumulated transversal and vertical displacement increments, associated with an arbitrary time $t_0 + \tau$, are determined from two coupled (but easily separable) simple first-order differential equations

$$\frac{dy^g}{dt} = v_c(UT, y^b, z^b) \quad (4)$$

$$\frac{dz^g}{dt} = w_c(UT, y^b, z^b) \quad (5)$$

associated with the initial conditions at the time of release

$$y^g(t_0) = 0; \quad \left. \frac{dy^g}{dt} \right|_{t=t_0} = v_c(UT, 0, 0) \quad (6)$$

*In a more complete model the effect on the wake deficit displacement, originating from *characteristic* u-turbulence components, could also be taken into account. In this case, the dynamics of a particular wake deficit release is not determined from the turbulence characteristics associated with a particular 'cross section' of the turbulence box, but depends on the turbulence characteristics in a, probably limited, 'region' of the turbulence box. As a consequence, the determination of the wake deficit 'trace' will require spatial interpolation in the longitudinal direction in the turbulence box. Further, and maybe more important, the determination of the instantaneous wake deficit will be coupled to the downstream wake advection in order to satisfy the along wind momentum balance. Finally, the transportation time of wake releases, between the wake generating rotor and a given downstream rotor, will vary from release to release, and special care must be taken to adjust/extend the length of the turbulence box in order to handle the wake releases whose dynamics is controlled by the end regions of the 'standard' turbulence box. Note, that the accuracy of the selected approximation increases as the rotor increases (cf. the definition of characteristic turbulence components in section *Filtering*).

and

$$z^g(t_0) = 0; \quad \left. \frac{dz^g}{dt} \right|_{t=t_0} = w_c(UT, 0, 0) \quad (7)$$

For a detailed description of the wake meander dynamics, we now consider a *cascade* of wake deficit releases. Thus, in addition to the initial release at time t_0 , releases are also performed at a number of supplementing time instants $t_i = t_0 + \Delta t_i$. The time evolution of these releases is described analogues to the release performed at time t_0 .

Because we have neglected the contribution from the along-wind turbulence component, the along-wind dynamics of these releases is invariant with respect to the emission time of those, meaning that each of these is advected downstream with the constant speed U .

The dynamics in a vertical plane is, however, release specific, because the transversal and vertical wake displacements are associated with different ‘cross sections’ of the turbulence box, and the wake releases thus most probably exposed to different (v, w) turbulent transport fields. For release times $t_i = t_0 + \Delta t_i$, the transversal and vertical displacement increments, at the arbitrary time $t_i + \tau$, are determined by integration of the following first-order differential equation system

$$\frac{dy^g}{dt} = v_c(U[T - t_i], y^b, z^b) \quad (8)$$

$$\frac{dz^g}{dt} = w_c(U[T - t_i], y^b, z^b) \quad (9)$$

associated with the following initial conditions at the time of release

$$y^g(t_i) = 0; \quad \left. \frac{dy^g}{dt} \right|_{t=t_i} = v_c(U[T - t_i], 0, 0) \quad (10)$$

and

$$z^g(t_i) = 0; \quad \left. \frac{dz^g}{dt} \right|_{t=t_i} = w_c(U[T - t_i], 0, 0) \quad (11)$$

As the wake deficit releases at the time instants $t_i = t_0 + \Delta t_i$ are associated with different ‘cross sections’ of the turbulence box, the *characteristics* of such deficits are also slightly different. This is because a given wake deficit depends on the instantaneous aerodynamic loading on the wind turbine rotor at the time of its release, and that the aerodynamic loading in turn depends on the total wind field including the turbulence characteristics, and thus the u component, which may easily vary between successive releases. Although the effect of the u -turbulence component presently is neglected in a wake *transport* context, the effect of the u -turbulence component on the wake deficit *generation* should be maintained.

Filtering

As mentioned in section *Basic Assumptions*, we consider wake meandering as being the result primarily of *large-scale* air movements, where the downstream evolution of the wake deficit position can be modelled, by considering the wake deficit as being a passive tracer transported in a large-scale turbulence field. As a consequence, we need an appropriate and consistent definition of the characteristic transversal and vertical wake transport velocities $v_c(x^b, y^b, z^b)$ and $w_c(x^b, y^b, z^b)$. These are achieved by introducing a low-pass filter in the turbulence description, extracting the requested transport velocities associated with the large-scale turbulent eddies. The cut-off frequency (in Hz), f_c , of the filtering may be specified as

$$f_c = \frac{U}{2D_w} \quad (12)$$

where D_w denotes the *instantaneous* wake deficit diameter, which will vary with the downstream transportation time.

The motivation for this choice is the following: a displacement-wave with period T_p has, because of the Taylor hypothesis, a spatial extend equal to UT_p . Thus, half of the spatial extend is associated with positive displacements, and the other half is associated with negative displacements. For a spatial structure, with a characteristic extend equal to a wake deficit diameter D_w , the minimum wave period, that allows for a constant sign displacement of all points on the spatial structure, is given by

$$D_w = \frac{UT_p}{2} \quad (13)$$

from which the selected cut-off frequency directly appears. The selected cut-off frequency corresponds to a spatial scale equal to $2D_w$, and the described filtering is thus equally well-obtained by averaging the (spatial) turbulence field over an area with the characteristic dimension $2D_w$. The selected averaging area, A_f , is most logically selected as a circle concentric with the advected wake deficit (i.e. with centre (y^b, z^b) and with a radius equal to D_w .

Denoting the (unfiltered) transversal and vertical turbulence components in the turbulence box by $v(x^b, y^b, z^b)$ and $w(x^b, y^b, z^b)$, respectively, the corresponding *characteristic* quantities are determined by

$$v_c(x^b, y^b, z^b) = \frac{1}{A_f} \iint_{A_f} v(x^b, y^b, z^b) dy^b dz^b \quad (14)$$

and

$$w_c(x^b, y^b, z^b) = \frac{1}{A_f} \iint_{A_f} w(x^b, y^b, z^b) dy^b dz^b \quad (15)$$

The present definition of the cut-off frequency is *not* unambiguous, as the requested large-scale segment of the turbulence eddies cannot be uniquely separated from the eddy scales mainly responsible for turbulence diffusion, and thus, wake expansion. Note, as indicated before, that the wake deficit diameter, D_w , appearing in the filter definitions (equations (14) and (15)), depends slightly on the downstream *transportation time*, as the wake expansion, caused by small-scale turbulence diffusion, depends on the time span, in which the diffusion process is active.

Numerical Scheme

The numerical scheme implemented for solving the first-order differential system defined in sections *Pseudo-Lagrangian Approach* and *Filtering*, respectively, are outlined in the following. Let us assume that the wake deficit releases (with slightly different characteristics depending on the rotor averaged u -turbulence component at the time of release) takes place at time instants $t_j = t_0 + j\Delta t$; $j = 0, \dots, N$, where $N = T/\Delta t$, and Δt is equal to the available (or selected) time resolution in the turbulence description. For each release, the differential equation system (equations (8)–(11)) is solved. The solution is determined by direct numerical integration in a loop containing the following steps:

- Initialize the problem using equations (10) and (11).
- Determine the characteristic transversal and vertical displacement velocities from equations (14) and (15) with filter characteristics being a function of transportation time *if* wake expansion is taking into account.
- Determine the wake position $(x_{k+1}^g, y_{k+1}^g, z_{k+1}^g)$ in iteration $(k + 1)$ as

$$\begin{aligned} x_{k+1}^g &= x_k^g + U\Delta t \\ y_{k+1}^g &= y_k^g + v_c(U[T - t_j], y_k^g, z_k^g)\Delta t \\ z_{k+1}^g &= z_k^g + w_c(U[T - t_j], y_k^g, z_k^g)\Delta t \end{aligned}$$

- Repeat the second and third items until $(k + 1) = N$.

Wake Dynamic at a Specific Downstream Distance

Let the solution to the differential equation system (8)–(11), for a wake deficit released at time t_i , be given by the displacement field $(x^g(t; t_i), y^g(t; t_i), z^g(t; t_i))$, and let us investigate the wake behaviour at the fixed downstream distance L_d . Given the model assumptions (constant wake advection velocity in the x^g direction), the transportation time between the point (i.e. cross section) of release and the downstream distance L_d is L_d/U . Thus, the centre of a wake deficit, released at time t_i , is positioned at $(x^g(L_d/U; t_i), y^g(L_d/U; t_i), z^g(L_d/U; t_i))$ at the downstream distance L_d .

In order to determine the *wake dynamics* as function of time, τ , at the downstream distance L_d , a ‘continuous’ release of wake deficits is considered. The resulting wake displacement field at the predefined downstream position, L_d , is thus given by $(L_d, y^g(L_d/U; t_0 + \tau), z^g(L_d/U; t_0 + \tau))$.

Simplification

The evaluation procedure described earlier can be somewhat simplified when the interest is restricted to the wake deficit behaviour at a given downstream distance from the wake generating wind turbine, *and if perfect correlation* between the *characteristic* transversal and vertical velocities in all ‘cross sections’ of the relevant turbulence box can be assumed. The latter condition essentially means that the characteristic turbulence components, associated with a given cross section of the turbulence box, are independent of the transversal and vertical coordinates. Central again is Taylor’s hypothesis relating the time dimension and the along-wind spatial dimension in a simple manner. According to Taylor, the (characteristic) velocities associated with the turbulence box coordinates (y_h^b, z_h^b) , i.e. the velocities along the line given by $(y^b, z^b) = (y_h^b, z_h^b)$, equal the (characteristic) velocities measured at a specific point fixed in space (for this application typically corresponding to the hub centre) where $(y^g, z^g) = (y_h^b, z_h^b)$, and the time scale relates to the spatial scale as $x^b = U\tau$.

When perfect correlation between *characteristic* transversal and vertical velocities in ‘cross sections’ of the turbulence box is presumed, a distinction between spatial points in a particular vertical ‘cross section’ of the turbulence box is meaningless. As a consequence, equations (8) and (9) degenerate to

$$\frac{dy^g}{dt} = v_c(U[T - t_i], 0, 0) \quad (16)$$

$$\frac{dz^g}{dt} = w_c(U[T - t_i], 0, 0) \quad (17)$$

Equations (16) and (17) describe the dynamics of *one* single wake release (released at time t_i). At the specified downstream distance L_d , the wake displacement, relative to the release position, is expressed as $(y^g, z^g) = L_d/U(v_c(U[T - t_i], 0, 0), w_c(U[T - t_i], 0, 0))$. For a continuous release of wake deficits, the resulting wake positions at the downstream distance L_d are in analogy determined by

$$(y^g, z^g) = \frac{L_d}{U}(v_c(U[T - t], 0, 0), w_c(U[T - t], 0, 0)) \quad (18)$$

or, if expressed in spatial coordinates

$$(y^g, z^g) = \frac{L_d}{U}(v_c(L - x^b, 0, 0), w_c(L - x^b, 0, 0)) \quad (19)$$

where the along-wind coordinate in the turbulence box, x^b , is restricted to the extend of the turbulence box in the mean wind direction (i.e. $x^b \in [0; L]$).

A priori, the simplification is believed to be a reasonable approximation for moderate downstream distances, where the wake centre displacements are modest, and where the change in the driving large-scale turbulence structures therefore also is moderate in the relevant spatial regime. For larger downstream distances, account should be taken to the spatial variability of the large-scale turbulence components, and the simplification consequently breaks down.

Reflecting Surface

The described large-scale eddy transport of the wake ‘centre of gravity’ may, at sufficiently large transportation times, result in a ‘collision’, and subsequent reflection, of part of the wake deficit from the ground surface. A simple model of this phenomenon is developed that, based on momentum balance, predicts a modified wake profile near the reflecting ground under these circumstances. The ground surface is assumed *plane* and *perfectly smooth* (frictionless), and the ambient velocity field is, consistently with the wake transport modelling, assumed constant and equal to the characteristic Taylor transport velocity, U .

In section *Basic Assumptions*, the close analogy between the proposed large-scale eddy wake deficit transport model and the traditional modelling of the transport of a passive tracer was pointed out. However, in the case of ground surface reflection, the modelling of these two physical mechanisms differs because of the variation in momentum inside a wake compared to the flow conditions associated with a passive tracer, where momentum is unaltered by the presence of the tracer. Therefore the simple concentration addition, applicable for passive tracers, must be replaced by a momentum balance consideration.

The proposed reflection model defines an unaltered wake deficit region and a modified wake deficit region (i.e. the region where reflection ‘superposition’ is taken place), and it ensures a smooth and continuous transition of the deficit velocities associated with the respective two regions. The distinction between the two wake deficit regions, as well as the deduction of the model, is described in details in Appendix.

The resulting expression for the deficit velocities in the modified wake region, $U_{wR}(y,z)$, is given by

$$U_{wR}(y, z) = U \left[1 - \sqrt{1 - \frac{C(y, z)}{U^2}} \right] \quad (20)$$

with $C(y,z)$ defined as

$$C(y, z) = U_w(y, z)[2U - U_w(y, z)] + U_w(y, -z)[2U - U_w(y, -z)] \quad (21)$$

and $U_w(y,z)$ being the unaltered deficit velocity field described in a wake deficit moving frame of reference, with $z = 0$ defining the ground surface.

In case of *small values* of $U_w(y,z)$, an asymptotic first-order expression of the modified wake deficit, $U_{wR}(y,z)$, can be developed. It turns out that this asymptotic expression is equivalent to what would result if the wake profile, in the wake reflection region, was considered as the result of a superposition of the physical wake ‘release’ field and an imaginary ‘release’ field located symmetrically to the actual release, but below the ground level, thus ensuring the correct boundary conditions at the ground level (no entrainment). Note that this result is equivalent to a simple plume reflection model for a passive tracer.

Implementation

Implementation of the developed wake meandering theory in a programme package, which allows for a practical employment, basically requires disposal of models for *wake deficit* prediction and for the *turbulent transport media*, respectively. The choices of these models are not unambiguous.

The wake model must, however, be formulated in the moving (meandering) frame of reference and preferably account for the wake expansion as function of downstream transportation time caused partly by turbulence diffusion and partly by the rotor pressure field. The resulting wake deficit will in the following be referred to as the *quasi-steady* wake deficit. In the wake-near field, the rotor pressure field is the main responsible for the wake expansion, whereas the turbulence diffusion gradually increases in importance with increasing downstream distance from the wake-generating turbine. Ideally, the turbulent wake diffusion should include diffusion contributions originating from the small-scale atmospheric turbulence as well as from the additional mechanically generated turbulence originating both from the wake shear field itself and from the mixing process taken place in the rotor plane.

The choice of a suitable turbulence field, that in turn defines the stochastic wake transport process, may be guided by the characteristics of the atmospheric turbulence at the site of relevance. These characteristics

encompass in principle not only turbulence standard parameters such as turbulence intensity, turbulence length scale, coherence properties, but also features like degree of isotropy, homogeneity of the turbulence, Gaussianity of the turbulence, etc.

The state-of-the-art implementation performed in the present context is based on an advanced wake deficit prediction model, involving a general purpose Navier–Stokes CFD code interfaced to an aeroelastic model.²¹ The 3D turbulence field modelling is based on the Mann model¹⁷ that combines rapid distortion theory, an assumed linear mean wind shear, the Von Kármán spectral tensor and a model for eddy lifetime. The basic features of these models are briefly described in the succeeding two sections. Note that, despite the apparent complexity of the programme package, the computational work associated with an aeroelastic computation, accounting for the meandering wake, is of the order of the resource requirements for a standard aeroelastic simulation of a turbulent load case, once the quasi-steady wake deficit has been determined.

Wake Deficit Modelling

The basic principle in the present wake deficit prediction is to couple a CFD actuator disc model of the rotor-wake interaction with an aeroelastic model. The motivation behind this strategy is the following: when substantial effort is to be devoted to obtain a detailed description of the wake flow field, it seems logical to model, as detailed as possible, the flow features of the ‘obstacle’ causing the wake (i.e. the actuator disc).

In brief, the idea is to calculate the induction, associated with the aerodynamic model of a wind turbine rotor in the aeroelastic model, by means of a 3D actuator disc model. In the present implementation, the flow solver is the general-purpose CFD program FIDAP,²² and the aeroelastic model is HAWC.²³ The overall strategy is as follows:

- An initial aeroelastic calculation is performed based on a traditional blade element momentum theory.
- The aerodynamic forces, resulting from this computation, are used to establish the first iteration of the actuator disc in the CFD model.
- The velocity field (in the rotor plane), resulting from an actuator disc CFD computation, is fed back as input to a new aeroelastic calculation, in which computation of induction in the aerodynamic model is omitted.
- The resulting aerodynamic forces are used to update the actuator disc model.

The third and fourth items are repeated until convergence is obtained. Using suitable relaxation between ‘new’ and ‘old’ aerodynamic forces, convergence is usually achieved within a few iterations.

For a given wake release at time t_i , the wind field at the rotor plane corresponds to the mean wind field superimposed on the turbulence, associated with a specific cross section of the synthetic turbulence box (cf. section *Pseudo-Lagrangian Approach*), and subsequently corrected in accordance with the associated induction velocities. However, in the present approach, the rotor turbulence loading is only treated approximately in the wake modelling, as the rotor disc turbulence field cannot easily be reproduced in the CFD model, and as a detailed CFD computation of all wake releases is too resource demanding for a suitable time discretization.

The selected approach is therefore the following:

- Initially wake deficits, corresponding to *five* suitable selected characteristic hub mean wind speeds (taking into account a prescribed mean wind shear profile), are computed.
- Subsequently, the hub mean wind speed, corresponding to a given release time, is determined as the *rotor averaged* value of the longitudinal turbulence component, associated with this particular release time, superimposed on the *rotor averaged* mean wind profile.
- Finally, the specific wake deficit, related to a particular release time, is determined accordingly by linear interpolation between the computed characteristic wake deficits.

In principle, the rotor averaged (v, w) turbulence components could also be taken into account in the determination of the wake deficits. However, that would require $5 \times 5 \times 5$ initial wake computations to set up the

interpolation scheme (five characteristic rotor averaged values for u , five characteristic rotor averaged values for v and five characteristic rotor averaged values for w).

In addition to wake meandering, the wake deficit dynamics includes *wake expansion* caused by the rotor pressure field, the rotor flow mixing and the (small to medium scale) turbulent diffusion because of the turbulence generated by the wake deficit shear, as well as to the ambient atmospheric turbulence. Adjusting the specific kinetic energy of the turbulence, $\frac{1}{2}\rho(u^2 + v^2 + w^2)$, in the CDF model suitable to the prescribed atmospheric turbulence, the wake expansion as function of transportation time can be approximated, in analogy with the determination of the initial wake (i.e. by interpolation in five wake expansion histories, each corresponding to characteristic values of the specific kinetic energy of the turbulence). Note, that adopting this refinement, the requested averaging area, A_f (cf. section *Filtering*), on which the characteristic transversal and vertical wake velocities are based, will depend on the actual transportation time of a particular wake deficit.

Atmospheric Turbulence

The large-scale advection of the wake deficit is essentially the wake meandering phenomenon. As described in section *Meandering Model*, the basic idea of the present model of the phenomenon, is successively to 'release' wake deficits from the wake-producing turbine into a turbulent wind field, and subsequently describe the dynamics of each of these releases. The applied 3D turbulence field, responsible for the advection of the individual wake releases, is a synthetic wind field based on either the Mann¹⁷ algorithm or the Shinozuka^{24,25} algorithm.

Whereas the Shinozuka method is based on one-point (cross-) spectra and two-point cross-spectra, the Mann method is based on a model of a spectral tensor for the atmospheric boundary layer (assuming neutral atmospheric stratification). Although the spectral tensor in principle contains the same information as the cross-spectra, the tensor formulation leads to considerable simpler and faster simulations of turbulence than the (more traditional) cross-spectra-based methods.

Traditionally, the fatigue loading of a turbine is determined based on aeroelastic calculations combining the load effect originating from a turbulence field as well as from a deterministic mean wind field (including tower wake effects and mean wind shear). In order to obtain a suitable frequency resolution, and at the same time limit the required computer resources (i.e. computational time and memory), the physical size (perpendicular to the mean wind direction) of the applied turbulence field is adjusted (i.e. is of the same size) to the actual rotor size. However, for the wake meandering modelling, only the large-scale turbulence eddies are of interest/relevance, and the physical size (perpendicular to the mean wind direction) of the required turbulence field for this application is increased to multiples of the rotor diameter, in order to be able to surround the wake movements downstream.

As a resource-saving alternative to the use of a large high-resolution turbulence grid, it was decided to apply two (independent) turbulence fields with different characteristic spatial scales. One turbulence field (covering only the rotor with conventional spatial grid resolution) is dedicated to the modelling of turbulence-generated fatigue loading, whereas the second turbulence field (with coarse spatial grid resolution, but having large spatial extend) is dedicated to the wake meandering modelling. The proposed approximation is almost 'exact', as very little correlation is expected between small- and large-scale turbulence components. Thus, essentially the only significant inaccuracy arises from the lack of correlation between the largest turbulence scales in the 'small' turbulence box and the smallest turbulence scales in the 'large' turbulence box.

An additional advantage of the 'two-box approach' is that the required spatial averaging, described in section *Filtering*, is automatically achieved when using the Mann turbulence generator, as the turbulence components, associated with a given turbulence grid point, is to be considered as spatial-averaged components over a unit grid resolution volume. If a Shinozuka-based turbulence algorithm is used, care must be taken to compute the requested area-averaged characteristic velocities, described in section *Filtering*, with sufficient statistical significance. If an area-averaging approach is selected, the requirements on the statistical significance might conflict with the preference of as few as possible simulation grid points. Therefore, preference must be given

to a time-filtering approach, in which the turbulence ‘time series’ of each grid point are low-pass filtered with a suitable cut-off frequency.

Another advantage with the Mann algorithm is that this model also provides an approximate simulation of a turbulence field bounded by a perfectly smooth ground surface. This facility is of particular relevance, when reflecting wake characteristics have to be considered, as it ensures that the movement of the wake deficit ‘centre of gravity’ will be bounded by the ground surface (cf. section *Reflecting Surface*). In short, the philosophy behind the approximate blocking facility is to superimpose, on a conventionally generated turbulence field, a pseudo-flow field with boundary conditions on the vertical flow component, along the blocking surface, as equal to minus the vertical turbulence component achieved from the conventional generated turbulence field. The resulting vertical flow component at the surface will thus equal zero.

The added pseudo-field assumes, as the conventional Mann model, linear wind shear, incompressible flow conditions ($\nabla \cdot \mathbf{u} = 0$, where \mathbf{u} denotes the pseudo-field), and allow for rotational flow conditions ($\nabla \times \mathbf{u} \neq 0$ in general). For large distances from the blocking surface, the difference between the blocked turbulence field and a conventional turbulence field is insignificant. However, as the distance to the blocking surface decreases, the effects manifest themselves gradually—the w -turbulence length scale decreases as well as the w -turbulence standard deviation, whereas the u - and v -turbulence standard deviations increase moderately.

Discussion of the Fundamental Meandering Mechanism

The fundamental assumption behind the developed theory is that the wake meandering process can be described as a series of consecutive wake ‘releases’, each advected downstream with the mean wind field and displaced, in the plane perpendicular to the mean wind direction, by the large-scale turbulence structures. In relation to the large-scale turbulence structures, the individual wake ‘releases’ are thus presumed to act like a passive tracer.

At first sight, the proposed wake meandering model seems to contradict results from recent wind tunnel studies, Medici and Alfredsson,²⁶ indicating that 3D low-frequency vortex shedding might control the wake meandering process. However, as we shall see, the contradiction is only seemingly, as there exists a number of notable differences between the experimental conditions obtained in the referred wind tunnel environment, and the conditions realized for a full-scale turbine located in the atmospheric boundary layer. First of all, the *loading* of a full-scale rotor is, under normal conditions, very different from the extremely high loading condition reported²⁶ for the rotor models. As increasingly high tip speed ratios of a rotor presents a decreasingly permeable disc to the flow, it is intuitively clear, that when the tip speed ratio is high enough, the rotor disc effectively becomes a solid plate,²⁷ where the flow, because of viscosity, separates at the disc’s edge. This observation is also in agreement with the results presented in Medici and Alfredsson,²⁶ as only tip speed ratios above approximately 3 were reported to generate vortex shedding. Secondly, the turbulence,* where added in the model studies, (most probably) failed to include the low-frequency part, claimed to be the main responsible for wake meandering mechanism in the atmospheric boundary layer, because it was created by a monoplane grid with a mesh width of only 50 mm (compared to a model rotor diameter of 180 mm), and further is confined by the wind tunnel cross-sectional dimensions. The turbulence produced by the applied monoplane grid will have a characteristic largest dimension of the order of 50 mm, and even though the rotor model is located at some downwind distance from the turbulence-generating grid,[†] the turbulent motions are known not to increase with downstream distance.²⁸

*In the absence of mean velocity gradients in the wind tunnel, the turbulence decays with downstream distance from turbulence-generating mechanism. For the present experiments, the turbulence intensity at the location of the model rotor is reported as 4.5%.

†The turbulence-generating grid is positioned 0.20 m downstream the inlet, whereas the rotor is positioned 1.45 m downstream the inlet.

Thus, the rhythmical vortex-shedding phenomenon reported in Medici and Alfredsson,²⁶ and further supported by a recent theoretical study of a laminar flow field by Okulov and Sørensen,²⁹ is believed to be associated with unrealistic loading conditions, compared to the loading situation of *full-scale* wind turbines located in the atmospheric boundary layer. This is further supported by the fact that substantial low-frequency tower reaction forces, associated with a possible rhythmic[‡] vortex-shedding phenomenon, have never been reported from full-scale load measurements. Moreover, the full-scale measurements from Tjæreborg, recorded at very low ambient turbulence intensity and analysed in Larsen *et al.*,¹ demonstrates a highly stable wake flow situation without any indications of vortex-shedding phenomena. Finally, preliminary analyses of a full-scale experiment, aiming at resolving the *instantaneous* wake deficit position behind a wind turbine using a 2D LiDAR measuring technique, strongly indicated the validity of the basic conjecture behind the proposed theory.^{30,31}

Conclusions

Wake meandering is of crucial importance in evaluation of *power production*[§] as well as of wind *turbine loading* in a wind turbine farm, and a simulation tool able to deal with this phenomenon is therefore highly desirable. We have developed a consistent, physical based theory for the wake meandering phenomenon. The model is at present confined to wake situations, where the wake in question does not interact with other wakes. The model does, however, include a simple heuristic description of wake interaction with a reflecting surface.

Whereas previous attempts to describe the wake meandering process and its consequences typically are empirically based and dedicated/fragmental, in the sense that the focus is *either* on power production *or* turbine (fatigue) loading, the present theory is *unifying*—describing the physical processes taken place—and thus encompasses both turbine power and load aspects. As for the turbine load aspects, the model is equally well-suited for estimation of fatigue loads as for estimation of extreme loads. As a consequence, the new wake meandering simulation philosophy, in addition to load and power estimates, also has an obvious potential for application in optimization of wind farm topology and wind farm operation, respectively, as well as in optimization of dedicated wind turbines for wind farm applications. Moreover, the new model can potentially be used for development of advanced control strategies for the individual turbine, in order to reduce the blade and turbine fatigue loading during wake operation.

The described wake meandering model is a crucial part of a newly developed integrated model complex for performing aeroelastic simulations of a wind turbine subjected to wake conditions, and the meandering model has been verified by comparing full-scale measurements with predictions obtained from this model complex.¹

In a future perspective, the fundamental assumption behind the present meandering theory will be further investigated, based on a newly developed full-scale 2D LiDAR measuring technique that allow for *instantaneous* recording of both transversal and vertical wake position and thus facilitating a direct resolution of the wake deficit displacement as function of time. Moreover, the present wake meandering description will be extended to allow for mutual interaction of two or more wakes, and the modified turbulence inside a meandering wake will be analysed and modelled.

[‡]With a non-dimensional frequency expressed as the Strouhal Number, $S_r = (fD)/U$, equal to approximately 0.12 according to Medici and Alfredsson²⁶, the physical distinct load frequency, f , associated with the vortex shedding, would be of the order 0.012 Hz for a $D = 80$ m rotor and a mean wind speed $U = 8$ m/s, whereas the frequency would be of the order 0.024 Hz for a wind speed $U = 16$ m/s.

[§]Compared to a simple statistical wake model based on superimposing steady state cases according to a probability density function the present approach will also include a power production contribution caused by the *dynamics* of the quasi-steady wake deficit. As an illustration, this dynamic contribution is in its character equivalent with the power production contribution originating exclusively from conventional turbulence for a given mean wind speed situation.

Acknowledgements

The Danish Energy Agency has funded part of the present work under the contract ENS 1364/04-0013. Further, stimulating discussions with our colleagues Morten Nielsen, and Jakob Mann at Risø National Laboratory for Sustainable Energy, Technical University of Denmark are acknowledged.

Appendix: Surface Reflection Model

The described large-scale eddy transport of the wake deficit ‘centre of gravity’ may, at sufficiently large transportation times, result in a ‘collision’, and subsequent reflection, of part of the wake deficit from the ground surface. A simple model of this phenomenon is described that, based on momentum balance,* predicts a modified wake deficit profile near the reflecting ground under these circumstances.

In general, the proposed model encompasses an unaltered wake deficit part and a modified wake deficit part (i.e. the region where reflection ‘superposition’ is taken place), and a smooth and continuous transition between these two parts is ensured.

The approach is in the present formulation restricted to the (dominating) along wind wake deficit component, but can easily be extended to account for other wake velocity components as well. Further, the ground surface is assumed *plane* and *perfectly smooth* (i.e. frictionless), and the ambient velocity field is assumed constant and equal to the mean wind speed U . Finally, we utilize that the static pressure in the wake at even moderate downstream distances is equal to the static pressure in the undisturbed part of the flow field.

Consider a cross section A-A of the trajectory of a (single) wake release, in which the wake deficit is defined within a region Ω (which does not need to hold any kind of symmetries, but can do) with the wake boundary $\delta\Omega$. In a Cartesian coordinate system, the wake deficit is denoted as $U_w(y,z)$ for $(y,z) \in \Omega$. The velocity field outside the wake region is assumed homogeneous with velocity U and equal to the velocity at the boundary $\delta\Omega$. The reflection is now defined by the position of the (plane) ground surface relative to the unaltered wake deficit, which, in the wake region Ω , is represented by a straight line l . The line l splits the original wake region in two parts—one, Ω_1 , representing the wake deficit above the ground surface, and another, Ω_2 , representing the (imaginary) wake deficit beneath the ground surface. Thus $\Omega = \Omega_1 \cup \Omega_2$. The situation is illustrated in Figure 3, showing a trajectory of a (single) wake release, and in Figure 4, showing the different wake regimes in cross section A-A.

The wake reflection mechanism is now presumed to be the following: The wake region is restricted to Ω_1 in case of reflection, and the direct influence on the wake deficit profile in Ω_1 , caused by the reflection, is restricted to a region Ω_{2R} of Ω_1 , where Ω_{2R} corresponds to Ω_2 mirrored in the line l . The wake deficit in the

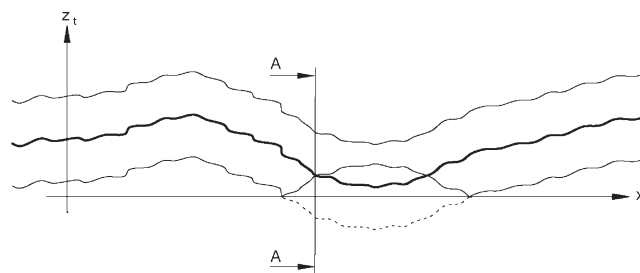


Figure 3. Wake trajectory for a (single) wake release

*Note the analogy between the described large-scale eddy wake deficit transport in section *Meandering Model* and the traditional modelling of the transport of a passive tracer. However, in case of ground reflection the modelling of these two physical mechanisms differ due to the variation in momentum inside a wake deficit compared to the flow conditions associated with a passive tracer, where momentum is unaltered by the presence of the tracer. Therefore the simple concentration addition, applicable for passive tracers, must be replaced by a momentum balance consideration.

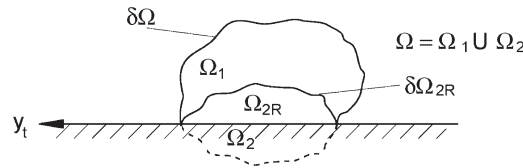


Figure 4. Wake cross-sectional regimes in section A-A

complement region $\Omega_1 \setminus \Omega_{2R}$ is thus *unaltered* by the reflection. The modified wake deficit in the region Ω_{2R} is defined in terms of the momentum balance described in the following.

Let the (modified) wake deficit in the region Ω_{2R} be denoted by $U_{wR}(y, z)$. Assuming homogeneous flow density and no recirculation, the momentum balance in the along wind direction pr. unit time is given by

$$\begin{aligned} & \rho \int_{\Omega_{2R}} [U - U_w(y, z)]^2 dy dz + \rho \int_{\Omega_2} [U - U_w(y, z)]^2 dy dz \\ &= \rho U^2 \int_{\Omega_2} dy dz + \rho \int_{\Omega_{2R}} [U - U_{wR}(y, z)]^2 dy dz \end{aligned} \quad (22)$$

The left-hand side of the momentum balance equation represents the momentum of the wake deficit before reflection is taken place. The right-hand side of the equation represents the momentum after reflection has occurred—first term is the (increased) momentum associated with a stream tube with a cross-sectional area corresponding to the ‘lost’ cross-sectional area of the deficit (i.e. the cross-sectional area of the imaginary deficit beneath the ground surface), and second term is the (decreased) momentum corresponding to the modified wake deficit in the intersection region Ω_{2R} .

We now introduce a variable transformation $(y, z) \rightarrow (y_t, z_t)$ that makes the y_t -axis coincide with the line l defining the reflection. The wake deficits in the transformed coordinates is denoted by $U_{wt}(y_t, z_t)$ and $U_{wRt}(y_t, z_t)$, respectively. Expressed in the transformed coordinates the momentum equation can be simplified to

$$\begin{aligned} & \rho \int_{\Omega_{2R}} [U - U_{wt}(y_t, z_t)]^2 dy_t dz_t + \rho \int_{\Omega_{2R}} [U - U_{wt}(y_t, -z_t)]^2 dy_t dz_t \\ &= \rho U^2 \int_{\Omega_2} dy_t dz_t + \rho \int_{\Omega_{2R}} [U - U_{wRt}(y_t, z_t)]^2 dy_t dz_t \end{aligned} \quad (23)$$

Utilizing that the cross-sectional area Ω_2 by definition equals the cross-sectional area Ω_{2R} , we finally arrive at

$$\int_{\Omega_{2R}} \{ [U - U_{wt}(y_t, z_t)]^2 + [U - U_{wt}(y_t, -z_t)]^2 - U^2 - [U - U_{wRt}(y_t, z_t)]^2 \} dy_t dz_t = 0 \quad (24)$$

To obtain the reflected wake shape, we finally assume that the above relation (24) is satisfied not only on integral basis, but also *locally*, i.e. that for $(y_t, z_t) \in \Omega_{2R}$

$$[U - U_{wt}(y_t, z_t)]^2 + [U - U_{wt}(y_t, -z_t)]^2 - U^2 - [U - U_{wRt}(y_t, z_t)]^2 = 0 \quad (25)$$

The assumption leading to equation (25) is essentially that the flow can be considered as *in-viscous* in the present context (in analogy to what is done in the blade element momentum theory for aerodynamic calculations), and further that the pressure can be considered *approximately constant* across cross sections perpendicular to the mean wind direction. Note that the neglected friction forces between infinitesimal stream surfaces are of the same order as the friction forces neglected in the blade element momentum theory, that often, in practical applications, defines the wake deficit in the rotor plane.

The interpretation of equation (25) is the following: For each infinitesimal area, $dA_t = dy_t, dz_t$, within Ω_{2R} , the momentum of the modified part of the reflected wake deficit is in balance with the momentum of the

corresponding infinitesimal cross-sectional area before reflection minus the difference in momentum corresponding to an increase of the imaginary flow velocity, of the imaginary mirrored (in the line l) infinitesimal cross-sectional area, from the wake flow velocity to the free stream velocity.

Based on equation (25), the (modified) wake deficit in the region Ω_{2R} is easily derived as

$$U_{wRl}(y_t, z_t) = U \left[1 - \sqrt{1 - \frac{C(y_t, z_t)}{U^2}} \right] \quad (26)$$

with $C(y_t, z_t)$ defined as

$$C(y_t, z_t) = U_{wt}(y_t, z_t)[2U - U_{wt}(y_t, z_t)] + U_{wt}(y_t, -z_t)[2U - U_{wt}(y_t, -z_t)] \quad (27)$$

Note that at the border of the modified wake region, $\delta\Omega_{2R}$, $U_{wt}(y_t, -z_t) = 0$ for $z_t > 0$, implying that $C(y_t, z_t) = U_{wt}(y_t, z_t)[2U - U_{wt}(y_t, z_t)]$ at $\delta\Omega_{2R}$ for $z_t > 0$, whereby $U_{wRl}(y_t, z_t) = U_{wt}(y_t, z_t)$ at $\delta\Omega_{2R}$ for $z_t > 0$. The described model thus ensures a *smooth and continuous transition* of the wake deficit between the unaffected wake region, $\Omega_1 \setminus \Omega_{2R}$, and the modified wake region, Ω_{2R} . Note further that $C(y_t, z_t) > 0$ as $U_{wRl}(y_t, z_t) < U$.

The momentum balance formulated in equations (22)–(25), and thus the above solution for the modified wake deficit in region Ω_{2R} , presumes that *no recirculation* takes place, i.e. that $U - U_{wRl}(y_t, z_t) > 0$. This assumption imposes a restriction on the maximal value of wake deficit, $U_{wt,max}(y_t, z_t)$. In relation to this discussion, the largest possible value of $U_{wt,max}(y_t, z_t)$, for which equation (26) still holds, is determined based on a (most critical) reflection situation where $U_{wt,max}(y_t, z_t)$ is lying on the line l defining the reflection. In this situation $z_t = 0$, and

$$C(y_t, z_t) = 2U_{wt,max}(y_t, 0)[2U - U_{wt,max}(y_t, 0)] \quad (28)$$

The resulting requirement on $U_{wt,max}(y_t, 0)$ is (cf. equation (26)) that

$$1 - \frac{C(y_t, z_t)}{U^2} \geq 0 \quad \text{or equivalently} \quad C(y_t, z_t) < U^2 \quad (29)$$

whereby we, by introduction of equation (28) into equation (29), arrive at

$$U_{wt,max}(y_t, 0) \leq U \left(1 - \frac{1}{\sqrt{2}} \right) \quad (30)$$

The requirement expressed in equation (30) states that as long as the maximum of a wake deficit is less than approximately $0.3U$, the described model is able to handle even the most critical reflection situation, where the wake deficit maximum is displaced to a position on the ground surface.

Under realistic turbulence conditions, the vertical displacement is traditionally somewhat less than the transverse displacement, and as a consequence the reflection situation will typically be associated with relatively large transportation times. Especially, the ‘most critical’ reflection situation described earlier will typically require quite large transportation times. For large transportation times, the wake expansion in turn results in reduced wake deficit amplitudes, and it is therefore believed that the model expressed in equations (26) and (27) covers most reflection situations of practical relevance.

However, under extreme turbulence conditions, the restriction introduced in equation (30) might be violated. For this reason, the model is extended in the following to take into account also a possible recirculation of (part of) the resulting reflected wake deficit. The starting point is the (local) momentum balance expressed in equation (25). According to equation (26), recirculation occurs when $C(y_t, z_t)$ exceeds U^2 . In order to include this situation,* the equation for the local momentum balance is therefore reformulated as

*The present modification of the reflection model assures that momentum equilibrium mathematically is maintained also in case of recirculation. However, it might be so that what in reality happens is that the momentum theory breaks down with the wake flow taking part of a mixing process, where air from outside the ‘reflection region’ is entrained to counteract reversal of the flow.

$$[U - U_{wt}(y_t, z_t)]^2 + [U - U_{wt}(y_t, -z_t)]^2 - U^2 - \text{sign}[U^2 - C(y_t, z_t)][U - U_{wRt}(y_t, z_t)]^2 = 0 \quad (31)$$

with $\text{sign}[*]$ denoting the sign operator. From equation (31), a general expression for the wake deficit in region Ω_{2R} , being able to handle possible recirculation situations, is derived and given as

$$U_{wRt}(y_t, z_t) = U \left\{ 1 - \text{sign}[U^2 - C(y_t, z_t)] \sqrt{\text{sign}[U^2 - C(y_t, z_t)] \left[1 - \frac{C(y_t, z_t)}{U^2} \right]} \right\} \quad (32)$$

with $C(y_t, z_t)$ defined according to equation (27).

In case of *small wake deficit* values, an asymptotic first-order expression of the modified wake deficit in reflection region Ω_{2R} can be derived. It turns out that this asymptotic expression is equivalent to what would result if the wake profile, in the wake reflection region, was considered as the result of a superposition of the physical wake ‘release’ and an imaginary ‘release’ located symmetrically to the actual release, but below the ground level, thus ensuring the correct boundary conditions at the ground level (no entrainment). This feature is, by the way, equivalent to the features of a simple plume reflection model.

The proof goes as follows. For small values of U_{wt} , the first-order approximation of $C(y_t, z_t)$ is given by

$$C(y_t, z_t) = 2U[U_{wt}(y_t, z_t) + U_{wt}(y_t, -z_t)] \quad (33)$$

whereby

$$\frac{C(y_t, z_t)}{U^2} = \frac{2[U_{wt}(y_t, z_t) + U_{wt}(y_t, -z_t)]}{U} \quad (34)$$

Small values of U_{wt} implies small values of $C(y_t, z_t)/U^2$, and a first-order Taylor expansion of equation (26) thus yields

$$U_{wRt}(y_t, z_t) = U \left[1 - \sqrt{1 - \frac{C(y_t, z_t)}{U^2}} \right] \approx U \left[1 - 1 + \frac{1}{2} \frac{C(y_t, z_t)}{U^2} \right] = U_{wt}(y_t, z_t) + U_{wt}(y_t, -z_t) \quad (35)$$

which shows that, in a first-order approximation, the proposed wake reflection model degenerates to a simple superposition of a physical and an imaginary wake release.

References

1. Larsen GC, Madsen HA, Bingöl F, Mann J, Ott S, Sørensen JN, Okulov V, Troldborg N, Nielsen M, Thomsen K, Larsen TJ, Mikkelsen R. Dynamic wake meandering modeling. *Risø-R-1607(EN)*. Risø National Laboratory: Roskilde, 2007.
2. Vermeulen PEJ. An experimental analysis of wind turbine wakes. In *Proceedings Third International Symposium on Wind Energy Systems, Lyngby, Denmark, August 1980*. Stephens HS, Stapleton CA (eds). BHRA Fluid Engineering: Cranfield, UK, 1980; 431–450.
3. Lissaman PBS. Energy effectiveness of arbitrary arrays of wind turbines. *AIAA Paper*, 79-0114, 1–7.
4. Ainslie JF. Development of an eddy viscosity model for wind turbine wakes. *Proceedings of the 7th British Wind Energy Association Conference*, Oxford, 27–29 March 1985; 61–66.
5. Taylor GJ, Milborrow DJ, McIntosh DN, Swift-Hokk DT. Wake measurements on the Nibe windmills. *Proceedings of the 7th British Wind Energy Association Conference*, Oxford, 27–29 March 1985; 67–74.
6. Ainslie JF. Wake modelling and the prediction of turbulence properties. *Proceedings of the 8th British Wind Energy Association Conference*, Cambridge, 19–21 March 1986; 115–120.
7. Ainslie JF. Calculating the flow field in the wake of wind turbines. *Journal of Wind Engineering & Industrial Aerodynamics* 1988; **27**: 213–224.
8. Högström U, Asimakopoulos DN, Kambezidis H, Helmis CG, Smedman A. A field study of the wake behind a 2 MW wind turbine. *Atmospheric Environment* 1988; **22**: 803–820.
9. Vermeer LJ, Sørensen JN, Crespo A. Wind turbine aerodynamics. *Progress in Aerospace Sciences* 2003; **39**: 467–510.
10. Thomsen K, Madsen HA, Larsen GC. *A New Method Can Predict Detailed Response for Turbines in Wind Farms*. Fact Sheet AED-RB-16(EN). Risø National Laboratory: Roskilde, 2003.
11. Madsen HA, Thomsen K, Larsen GC. A new method for prediction of detailed wake loads. In *Proceedings of IEA Joint Action of Wind Turbines 16th Symposium, Boulder, CO, May 2003, NREL*. Thor S-E (ed.). FOI, Aeronautics-FFA: Stockholm, Sweden, 2003; 171–188.

12. Thomsen K, Madsen HA. A new simulation method for turbine in wakes—applied to extreme response during operation. *Wind Energy* 2005; **8**: 35–47.
13. Frandsen S. *Turbulence and Turbulence Generated Fatigue Loading in Wind Turbine Clusters*. Risø-R-1188(EN). Risø National Laboratory: Roskilde, 2003.
14. IEC TC88-MT1 (ed.). *IEC 61400-1 Ed.3 CD. 2. Revision. Wind Turbines. Part 1: Design Requirements*. International Electrotechnical Commission: Geneva, Switzerland, 2005.
15. Abramovich GN. *The Theory of Turbulent Jets*. MIT Press: Cambridge, 1963.
16. Fox RW, McDonald AT, Pritchard PJ. *Introduction to Fluid Mechanics*. John Wiley & Sons: Hoboken, 2006.
17. Mann J. The spatial structure of neutral atmospheric surface-layer turbulence. *Journal of Fluid Mechanics* 1994; **273**: 141–168.
18. L'vov VS, Pomyalov A, Procaccia I. Temporal surrogates of spatial turbulent statistics: the Taylor hypothesis revised. *Physical Review E* 1999; **60**: 4175–4184.
19. Krogstad PÅ, Kaspersen JH, Rimestad S. Convection velocities in a turbulent boundary layer. *Physics of Fluids* 1998; **10**: 949–957.
20. Panofsky HA, Dutton JA. *Atmospheric Turbulence—Models and Methods for Engineering Applications*. John Wiley & Sons, 1984.
21. Madsen HA. (ed.) *Research in Aeroelasticity*. Risø-1129(DA). Risø National Laboratory: Roskilde, 1999. (In Danish)
22. FIDAP8. *FIDAP User's Manual*. Fluent Inc.: Lebanon, NH (USA), 1998.
23. Thirstrup Petersen J. *Kinematically Nonlinear Finite Element Model of a Horizontal Axis Wind Turbine*. Parts 1 and 2. Risø National Laboratory: Roskilde, 1990.
24. Shinozuka M, Jan CM. Digital simulation of random processes and its applications. *Journal of Sound and Vibration* 1972; **25**: 111–128.
25. Veers PS. *Three Dimensional Wind Simulation*. SAND88-0152. Sandia National Laboratories: Albuquerque, 1988.
26. Medici D, Alfredsson PH. Measurements on a wind turbine wake: 3D effects and bluff-body vortex shedding. The science of making torque from wind. *Special Topic Conference*, Delft, 19–21 April 2004; 155–165.
27. Burton T, Sharpe D, Jenkins N, Bossanyi E. *Wind Energy Handbook*. John Wiley & Sons: Chichester, 2001.
28. Pope SB. *Turbulent Flows*. Cambridge University Press: New York, 2000.
29. Okulov VL, Sørensen JN. Stability of helical tip vortices in a rotor far wake. *Journal of Fluid Mechanics* 2007; **576**: 1–25.
30. Bingöl F, Mann J, Larsen GC. Laser measurements of wake dynamics (invited paper and presentation). *Scientific Proceedings. 2007 European Wind Energy Conference and Exhibition*, Milan, 7–10 May 2007; 103–106.
31. Bingöl F, Larsen GC, Mann J. Wake meandering—an analysis of instantaneous 2-D laser measurements. *Proceedings of the Second Conference on the Science of Making Torque from Wind*, Technical University of Denmark, Lyngby, 28–31 August 2007.